

Research Article

Applications of Symmetric and Nonsymmetric MSSOR Preconditioners to Large-Scale Biot's Consolidation Problems with Nonassociated Plasticity

Xi Chen¹ and Kok Kwang Phoon²

¹ *Department of Geotechnical Engineering, School of Civil Engineering, Beijing Jiaotong University, Beijing 100044, China*

² *Department of Civil and Environmental Engineering, National University of Singapore, E1A-07-14, Blk E1A, 07-03, 1 Engineering Drive 2, Singapore 117576*

Correspondence should be addressed to Xi Chen, chenxi@bjtu.edu.cn
and Kok Kwang Phoon, kkphoon@nus.edu.sg

Received 12 October 2011; Revised 14 December 2011; Accepted 15 December 2011

Academic Editor: Massimiliano Ferronato

Copyright © 2012 X. Chen and K. K. Phoon. This is an open access article distributed under the Creative Commons Attribution License, which permits unrestricted use, distribution, and reproduction in any medium, provided the original work is properly cited.

Two solution schemes are proposed and compared for large 3D soil consolidation problems with nonassociated plasticity. One solution scheme results in the nonsymmetric linear equations due to the Newton iteration, while the other leads to the symmetric linear systems due to the symmetrized stiffness strategies. To solve the resulting linear systems, the QMR and SQMR solver are employed in conjunction with nonsymmetric and symmetric MSSOR preconditioner, respectively. A simple footing example and a pile-group example are used to assess the performance of the two solution schemes. Numerical results disclose that compared to the Newton iterative scheme, the symmetric stiffness schemes combined with adequate acceleration strategy may lead to a significant reduction in total computer runtime as well as in memory requirement, indicating that the accelerated symmetric stiffness method has considerable potential to be exploited to solve very large problems.

1. Introduction

The wide applications of large-scale finite element analyses for soil consolidation settlements demand efficient iterative solutions. Among various iterative solvers the Krylov subspace iterative methods have enjoyed great popularity so that it was ranked as one of top ten algorithms invented in the 20th century [1]. In large-scale finite element computations, the success of Krylov subspace iterative methods may be partially attributed to the matrix-vector

multiplications which can be implemented sparsely in the iterative process, but it is the preconditioning technique that makes Krylov subspace iterative methods become practically useful.

For an indefinite linear system some preconditioning methods (such as incomplete LU or ILU) originally proposed for general problems may encounter slow convergence or even breakdown during the iterative process (e.g., [2]). In the past decade, many researchers have focused on constructing preconditioners for indefinite problems either by revising a standard preconditioner or by designing a block preconditioner according to the block matrix structure. For example, for the indefinite linear equation stemming from Biot's consolidation a generalized Jacobi (GJ) preconditioner was proposed by Phoon et al. [3] to overcome the unbalanced diagonal scaling of standard Jacobi, while to obviate unstable triangular solves a modified symmetric successive overrelaxation (MSSOR) preconditioner [4] was designed to enhance the pivots embedded within the standard symmetric successive overrelaxation (SSOR) factorization. The successes of GJ and MSSOR undoubtedly are attributed to the fact that both of them were developed based on the block matrix structure. On a separate track, many other researchers have been working on block preconditioners. Perugia and Simoncini [5] proposed symmetric indefinite block diagonal preconditioners for mixed finite element formulations, and, furthermore, Simoncini [6] proposed block triangular preconditioners to couple with symmetric quasiminimal residual (SQMR) [7] for symmetric saddle-point problems. Keller et al. [8] and Bai et al. [9] developed their own block constraint preconditioners for indefinite linear systems. For three types of block preconditioners, an in-depth comparison and eigenvalue study has been carried out by Toh et al. [10], and it was concluded that the block constraint preconditioner and the diagonal GJ preconditioner could be more promising for large-scale Biot's linear system. Recently, more attentions have been paid to the constraint block structure. For instance, Bergamaschi et al. [11], Ferronato et al. [12], and Haga et al. [13] defined their own block constraint preconditioners, respectively, and validated the good performance of their block constraint preconditioners. Furthermore, Janna et al. [14] developed a parallel block preconditioner for symmetric positive definite (SPD) matrices by coupling the generalized factored sparse approximate inverse (FSAI) with ILU factorization, and it was concluded that in many realistic cases the FSAI-ILU preconditioner is more effective than both FSAI and ILU preconditioners. To resolve the soil-structure problems in which material stiffness contrast is significant, the partitioned block diagonal preconditioners were proposed by Chaudhary [15], and numerical results indicate that the proposed preconditioners are not sensitive to the material stiffness contrast ratio. Based on the above review, it seems that constructing a preconditioner based on the block structure of the coefficient matrix has become a popular strategy for large-scale Biot's indefinite linear systems.

Soil consolidation accompanied with soil dilatancy may be frequently encountered in practice, and commonly the soil dilatancy may be modeled by nonassociated plasticity. The main contribution of the article is that for coupled consolidation problems involving nonassociated plasticity, two solution strategies are proposed and evaluated, respectively, by employing a strategy of combining a nonlinear iterative scheme with a corresponding linear iterative method (e.g., [16, 17]). The paper is organized as follows. In Section 2, the nonlinear iterative methods are formulated for elastoplastic soil consolidation problems, and the coupled 2×2 nonsymmetric indefinite Biot's finite element linear system of equation due to nonassociated plastic flow is derived. In Section 3, the recently proposed block preconditioners are reviewed and commented. In Section 4, both symmetric version and nonsymmetric

version of MSSOR are implemented within the proposed two schemes, respectively, to solve the soil consolidation examples with nonassociated plasticity, and their performances are investigated and compared. Finally, some useful observations and conclusions are summarized in Section 5.

2. Coupled Linear System of Equation Arising from Elastoplastic Biot's Consolidation Problems

Soil consolidation is a soil settlement process coupled with dissipation of excess pore water pressure, and this process may be physically modeled by the widely accepted Biot's consolidation theory [18]. Recall that for a fully saturated porous media, the volumetric fluid content variation within the soil skeleton is solely related to the deformation of solid skeleton, that is,

$$\nabla \cdot \boldsymbol{\sigma}(\mathbf{x}, t) - \gamma \mathbf{b} = 0, \quad (\mathbf{x}, t) \in \Omega \times (0, T], \quad (2.1)$$

in which the Terzaghi's effective stress principle $\boldsymbol{\sigma} = \boldsymbol{\sigma}' + p$ is applied; $\mathbf{b} = [0, 0, 1]^T$ is the unit body force vector; γ is the total unit weight; Ω is the solution domain; T is the total analyzing time. For the fully saturated porous media, the pore fluid should comply with the fluid continuity equation or the mass-conservation equation, that is,

$$\nabla \cdot \dot{\mathbf{u}}(\mathbf{x}, t) + \nabla \cdot \mathbf{v}_f(\mathbf{x}, t) = 0, \quad (2.2)$$

where $\nabla \cdot \dot{\mathbf{u}} = \dot{\varepsilon}_v$ with ε_v as the volumetric strain, the dot symbol over any symbols means time differentiation, and \mathbf{u} is the displacement vector; the fluid velocity \mathbf{v}_f is described by Darcy's law

$$\mathbf{v}_f = -\frac{[\mathbf{k}]}{\gamma_f} (\nabla p - \gamma_f \mathbf{b}). \quad (2.3)$$

Here, γ_f is the unit weight of pore fluid; $[\mathbf{k}] = [\mathbf{k}_s]$ is the hydraulic conductivity tensor (it is a diagonal matrix $[\mathbf{k}_s] = \text{diag}(k_{s,x}, k_{s,y}, k_{s,z})$ when orthogonal hydraulic conductivity properties are assumed) for saturated flow. The solution domain Ω has the complementary boundary conditions may be given as $\partial\Omega = \partial\Omega_D \cup \partial\Omega_N$ and $\partial\Omega_D \cap \partial\Omega_N = \emptyset$ with $\partial\Omega_D$ for the Dirichlet (or prescribed displacement and pore pressure) boundary and $\partial\Omega_N$ for the Neumann (or prescribed force and flux) boundary. After discretizing (2.1) and (2.2) in space and time domain, respectively, the incremental form of Biot's finite element equation is derived as (e.g., [19]):

$$\begin{bmatrix} \mathbf{K} & \mathbf{L} \\ \mathbf{L}^T & -\theta \Delta t \mathbf{G} \end{bmatrix} \begin{Bmatrix} \Delta \mathbf{u} \\ \Delta \mathbf{p}^{ex} \end{Bmatrix} = \begin{Bmatrix} \Delta \mathbf{f} \\ \Delta t \mathbf{G} \mathbf{p}_n^{ex} \end{Bmatrix} \quad (2.4)$$

in which the subblocks within the coupled matrix are defined, respectively, as

$$\begin{aligned}\mathbf{K} &= \sum_e \left(\int_{V_e} \mathbf{B}_u^T \mathbf{D}_{ep} \mathbf{B}_u dV \right), \\ \mathbf{L} &= \sum_e \left(\int_{V_e} \mathbf{B}_u^T \mathbf{1} \mathbf{N}_p dV \right), \\ \mathbf{G} &= \sum_e \left(\int_{V_e} \mathbf{B}_p^T \frac{[\mathbf{k}]}{\gamma_f} \mathbf{B}_p dV \right),\end{aligned}\quad (2.5)$$

where \mathbf{D}_{ep} is the constitutive matrix; \mathbf{B}_u , \mathbf{B}_p is the gradient of shape function \mathbf{N}_u and \mathbf{N}_p used for interpolating the displacement \mathbf{u} and the excess pore pressure \mathbf{p}^{ex} , respectively; $\mathbf{1} = [1 \ 1 \ 1 \ 0 \ 0 \ 0]^T$; Δt is the time increment; θ is the time integration parameter ranging from 0 to 1; $\theta = 1/2$ corresponds to the second-order accuracy Crank-Nicolson method, while $\theta = 1$ leads to the fully implicit method possessing the first-order accuracy.

Equation (2.4) is the discretized finite element equation for each time increment, and to be convenient the following weak form of the residual equation is used to derive the nonlinear iterative process,

$$\mathbf{R}(\mathbf{u}; \mathbf{p}^{ex}) = \begin{bmatrix} \mathbf{R}_u \\ \mathbf{R}_p \end{bmatrix} = \begin{bmatrix} \mathbf{F}_u^{\text{ext}} \\ \mathbf{F}_p^{\text{ext}} \end{bmatrix} - \begin{bmatrix} \mathbf{F}_u^{\text{int}} \\ \mathbf{F}_p^{\text{int}} \end{bmatrix} = \begin{bmatrix} \mathbf{0} \\ \mathbf{0} \end{bmatrix}, \quad (2.6)$$

where \mathbf{R} is the residual or out-of-balance force vector derived from the total potential energy $\Phi(\mathbf{u}; \mathbf{p}^{ex})$; \mathbf{F}^{ext} is the applied external force at current time increment, and its two parts corresponding to \mathbf{u} and \mathbf{p}^{ex} , respectively, have been presented in the RHS of (2.4). Noting that the deformation of soil skeleton is solely caused by the effective stress, the internal forces $\mathbf{F}_u^{\text{int}}$ and $\mathbf{F}_p^{\text{int}}$ may be expressed, respectively, as below,

$$\begin{aligned}\mathbf{F}_u^{\text{int}} &= \int_V \mathbf{B}_u^T \boldsymbol{\sigma}' dV + \int_V \mathbf{B}_u^T \mathbf{p}^{ex} dV, \\ \mathbf{F}_p^{\text{int}} &= \int_V \mathbf{N}_p^T \boldsymbol{\varepsilon} dV + \theta \Delta t \int_V \mathbf{B}_p^T \mathbf{v}_f dV.\end{aligned}\quad (2.7)$$

Applying the first-order Taylor expansion to (2.6) leads to the following Newton-Raphson (NR) iteration:

$$\mathbf{R}(\mathbf{u}_{k-1}; \mathbf{p}_{k-1}^{ex}) + \mathbf{A}_{k-1} \begin{bmatrix} \delta \mathbf{u}_k \\ \delta \mathbf{p}_k^{ex} \end{bmatrix} = 0, \quad (2.8)$$

$$\begin{bmatrix} \mathbf{u}_k \\ \mathbf{p}_k^{ex} \end{bmatrix} = \begin{bmatrix} \mathbf{u}_{k-1} \\ \mathbf{p}_{k-1}^{ex} \end{bmatrix} + \begin{bmatrix} \delta \mathbf{u}_k \\ \delta \mathbf{p}_k^{ex} \end{bmatrix}, \quad (2.9)$$

where

$$\mathbf{A}_{k-1} = \begin{bmatrix} \left. \frac{\partial \mathbf{R}_u}{\partial \mathbf{u}} \right|_{k-1} & \frac{\partial \mathbf{R}_u}{\partial \mathbf{p}^{ex}} \\ \frac{\partial \mathbf{R}_p}{\partial \mathbf{u}} & \frac{\partial \mathbf{R}_p}{\partial \mathbf{p}^{ex}} \end{bmatrix}, \quad \frac{\partial \mathbf{R}_u}{\partial \mathbf{p}^{ex}} = \left[\frac{\partial \mathbf{R}_p}{\partial \mathbf{u}} \right]^T = -\mathbf{L}, \quad \frac{\partial \mathbf{R}_p}{\partial \mathbf{p}^{ex}} = \theta \Delta t \mathbf{G} \quad (2.10)$$

in which it is apparent that \mathbf{L} is independent of time increment and iterative process due to small-strain finite element computation, and \mathbf{G} is independent of time increment and iterative process due to the saturated soil assumption. In \mathbf{A}_{k-1} , the gradient of \mathbf{R}_u about \mathbf{u} is the tangential solid stiffness matrix,

$$\mathbf{K}_T = -\frac{\partial \mathbf{R}_u}{\partial \mathbf{u}} = \frac{\partial \mathbf{F}_u^{\text{int}}(\mathbf{u})}{\partial \mathbf{u}}, \quad (2.11)$$

and \mathbf{K}_T is assembled by the element stiffness \mathbf{k}_{ep} , that is,

$$\mathbf{K}_T = \sum_{\text{elements}} \frac{\partial (\int_{V_e} \mathbf{B}^T \mathbf{D}_{ep} \mathbf{B} dV \mathbf{u}_e)}{\partial \mathbf{u}} = \sum_{\text{elements}} \mathbf{k}_{ep} \quad \text{with } \mathbf{k}_{ep} = \int_{V_e} \mathbf{B}^T \mathbf{D}_{ep} \mathbf{B} dV. \quad (2.12)$$

Evidently, the symmetry of \mathbf{K}_T or the 2×2 coupled matrix \mathbf{A}_{k-1} in (2.10) is governed by \mathbf{D}_{ep} , which may be expressed as

$$\mathbf{D}_{ep} = \mathbf{D}_e - \mathbf{D}_p = \mathbf{D}_e - \frac{\mathbf{D}_e \mathbf{b} \mathbf{a}^T \mathbf{D}_e}{\mathbf{a}^T \mathbf{D}_e \mathbf{b} - \mathbf{c}^T \mathbf{h}}, \quad (2.13)$$

where $\mathbf{a} = \partial_\sigma F$ represents the yield surface normal vector, $\mathbf{b} = \partial_\sigma G$ denotes the plastic flow direction vector, while $\mathbf{c} = \partial_q F$ is the gradient of yield function (i.e., F) about the internal variables of the soil model. In conventional elastoplastic soil models, the physically associated plastic flow leads to symmetric \mathbf{D}_{ep} due to $\mathbf{b} = \mathbf{a}$, while the nonassociated plastic flow results in nonsymmetric \mathbf{D}_{ep} due to $\mathbf{b} \neq \mathbf{a}$. For convenience, (2.8) may be further expressed as

$$\begin{bmatrix} \mathbf{K}_{k-1} & \mathbf{L} \\ \mathbf{L}^T & -\theta \Delta t \mathbf{G} \end{bmatrix} \begin{Bmatrix} \delta \mathbf{u} \\ \delta \mathbf{p}^{ex} \end{Bmatrix}_k = \mathbf{R}_{k-1} = \mathbf{F}^{\text{ext}} - \mathbf{F}_{k-1}^{\text{int}}, \quad (2.14)$$

where the superscript k signifies the nonlinear iteration count within each time increment. To distinguish the nonlinear iterative process from the Krylov subspace iterative process, the iteration count for the first process as described by (2.14) is called nonlinear iteration count, while the second Krylov subspace process is a linear iterative process, and the iteration count for this process is called linear iteration count.

In the nonlinear iterative process, the search direction \mathbf{d}_k may be computed inexactly (i.e., $\mathbf{d}_k \approx [\delta \mathbf{u}; \delta \mathbf{p}^{ex}]_k^T$), leading to the so-called inexact Newton method whose convergence is governed by (e.g., [16, 17]),

$$\|\mathbf{R}_{k-1} + \mathbf{A}_{k-1} \mathbf{d}_k\| \leq \eta_{k-1} \|\mathbf{R}_{k-1}\|, \quad (2.15)$$

where $\eta_{k-1} \in [0, 1)$ is the forcing term. With the computed search direction \mathbf{d}_k , the displacement is updated by

$$\begin{bmatrix} \mathbf{u}_k \\ \mathbf{p}_k^{ex} \end{bmatrix} = \begin{bmatrix} \mathbf{u}_{k-1} \\ \mathbf{p}_{k-1}^{ex} \end{bmatrix} + \chi_k \begin{bmatrix} \delta \mathbf{u}_k \\ \delta \mathbf{p}_k^{ex} \end{bmatrix} \quad (2.16)$$

in which χ_k is the step-length parameter, which may be determined by some optimization strategies. The inexact computation of \mathbf{d}_k may arise from the approximate solve of \mathbf{d}_k or the approximation to \mathbf{A}_{k-1} .

For ease of presentation, the linear system of equation at each nonlinear iteration as shown by (2.14) is expressed concisely as

$$\begin{bmatrix} K & B \\ B^T & -C \end{bmatrix} \begin{Bmatrix} x \\ y \end{Bmatrix} = \begin{Bmatrix} f \\ g \end{Bmatrix} \quad \text{with } A = \begin{bmatrix} K & B \\ B^T & -C \end{bmatrix}_{N \times N}. \quad (2.17)$$

3. Block-Structured Preconditioners

Here, the block-structured preconditioners are defined as those developed according to the coefficient matrix block structure, and hence they include the block preconditioners and those modified preconditioners inspired by the matrix block structure.

3.1. Block Preconditioners for Biot's Linear System of Equation

Block preconditioners can be classified into three types as mentioned previously. According to Toh et al. [10], it could be convenient to derive the preconditioners based on the matrix inverse. Note that the inverse of the 2×2 matrix in (2.17) may be expressed as

$$\begin{bmatrix} K & B_2 \\ B_1^T & -C \end{bmatrix}^{-1} = \begin{bmatrix} K^{-1} - K^{-1}B_2S^{-1}B_1^TK^{-1} & K^{-1}B_2S^{-1} \\ S^{-1}B_1^TK^{-1} & -S^{-1} \end{bmatrix} \quad (3.1)$$

in which $S = C + B_1^TK^{-1}B_2$ (with $B_1 = B_2$) is the Schur complement matrix. Given a vector $[u; v]$ and a block preconditioner $M \approx A$ with the approximation \hat{K} and \hat{S} to K and S , respectively. Hence, the preconditioning step may be written as the following.

Preconditioning Step $M^{-1}[u; v]$:

$$\text{solve } p = \hat{K}^{-1}u,$$

$$\text{solve } q = \hat{S}^{-1}(B_1^T p - v),$$

$$\text{compute } M^{-1}[u, v]^T = [\hat{K}^{-1}(u - B_2q); q].$$

The above preconditioning step has already been introduced in [4, 10] for the block constraint preconditioners; however, it is highlighted here as a unified computational framework for all block preconditioners. It can be observed that within the above preconditioning step, canceling the terms associated with off-diagonal subblocks B_1 and B_2 corresponds

Table 1: Block preconditioners recently proposed for Biot's linear system.

Authors	Type	Block preconditioner	
		\hat{K}	\hat{S}
Phoon et al. [3]	Diagonal	Diag(K)	diag[$C + B^T \text{diag}(K)^{-1}B$]
		Direct inverse	Direct inverse
Simoncini [6]	Triangular	K	$C + B^T B$
		Incomplete Cholesky	Incomplete Cholesky
Toh et al. [10]	All three types	diag(K)	$C + B^T \hat{K}^{-1}B$
		Direct inverse	Incomplete or sparse Cholesky
Bergamaschi et al. [11]	Constraint	$L_K L_K^T \& (ZZ^T)^{-1}$	$C + B^T \hat{K}^{-1}B$
		Incomplete Cholesky and approximate inverse	Incomplete Cholesky
Haga et al. [13]	Constraint	diag(K) & K	diag[$C + B^T \text{diag}(K)^{-1}B$] & $C + B^T \text{diag}(K)^{-1}B$
		AMG	Direct inverse & AMG
Chaudhary [15]	Diagonal	Partitioned block diagonal	diag[$C + B^T \text{diag}(K)^{-1}B$]
		Cholesky & direct inverse	Direct inverse

to the block diagonal preconditioning, while canceling either B_1 or B_2 corresponds to the block triangular types. Depending on how \hat{K} and \hat{S} are approximated, various block preconditioners may be developed. Regardless of the type of preconditioners adopted, solving the linear systems associated with \hat{K} and \hat{S} can not be obviated. Consequently, how \hat{K} and \hat{S} are approximated and how these linear systems are solved efficiently are the key features distinguishing recently proposed block preconditioners. For example, Phoon et al. [3] proposed the diagonal approximations to both \hat{K} and \hat{S} so that the inverses of \hat{K} and \hat{S} can be directly attained. While in the block constraint preconditioner proposed by Toh et al. [10], because it is observed that the size of K is significantly larger than that of S , a diagonal approximation is employed for K , and the incomplete or sparse Cholesky factorization is recommended for \hat{S} . In another version of block constraint preconditioner proposed by Bergamaschi et al. [11, 12], the incomplete Cholesky factorization and factorized approximate inverse are adopted for \hat{K} and \hat{S} , respectively. Different from the previous studies, Haga et al. [13] recommended solving the linear systems \hat{K} and \hat{S} using the algebraic multigrid (AMG) method. To summarize the key differences, these block preconditioners with the proposed \hat{K} and \hat{S} as well as the corresponding solution schemes are tabulated in Table 1. In the table, all block preconditioners are categorized into three types including the block diagonal preconditioners, block triangular preconditioners, and block constraint preconditioners which are denoted as "diagonal," "constraint," and "triangular," respectively.

3.2. Modified Preconditioners Based on Matrix Block Structure

There are some advantages to developing preconditioners based on the matrix block structure, particularly in the case of block indefinite linear systems. It is natural to hope that modifying some standard or general preconditioning techniques may lead to improved versions. For instance, the generalized Jacobi preconditioner [3] may be viewed as an

improved version of standard Jacobi preconditioner by referring to the block diagonal. The MSSOR preconditioner [4] may also be regarded as a good example that demonstrates how to develop a preconditioner based on a standard preconditioner to suit indefinite problems. The general nonsymmetric form of MSSOR may be expressed as below

$$M_{\text{MSSOR}} = \left(L_A + \frac{D}{\omega} \right) \left(\frac{D}{\omega} \right)^{-1} \left(U_A + \frac{D}{\omega} \right) = \left(L_A + \tilde{D} \right) \tilde{D}^{-1} \left(U_A + \tilde{D} \right), \quad (3.2)$$

where $\omega \in [1, 2]$ is the relaxation parameter; L_A, U_A is the strictly lower and upper part of matrix A , respectively, that is, $A = L_A + U_A + D_A$. For symmetric linear equation, $L_A = U_A^T$ leads to the symmetric MSSOR. D is the modified diagonal and it is recommended to take GJ, that is,

$$D = M_{\text{GJ}} = \begin{bmatrix} \text{diag}(K) & 0 \\ 0 & \alpha \text{diag}(\hat{S}) \end{bmatrix} \quad (3.3)$$

in which α is a scaling factor which is recommended to be -4 according to the eigenvalue study. It is clear that MSSOR preconditioner can be implemented efficiently when combined with the Eisenstat trick [20]. In the following part, both symmetric version and nonsymmetric version of MSSOR preconditioner will be employed for large-scale nonlinear soil consolidation involving nonassociated plasticity.

4. Numerical Experiments

To simulate soil dilatancy during the soil consolidation process, an elastoplastic soil model with nonassociated plasticity should be used [21]. The nonassociated plasticity theory is a generalization of the classical elastoplastic theory by introducing a new plastic potential function [22], and in the past decades the nonassociated plasticity theory is widely applied in practical finite element analyses.

It is also well known that when the nonassociated plastic soil models are employed in finite element analysis, the resulting linear systems of equations are nonsymmetric. Solving the linear equations separately from the nonlinear iterative procedure may not be wise, because an appropriate combination between the outer nonlinear iterative scheme and an inner linear iterative solution may lead to a significant reduction in computer runtime without sacrificing accuracy [17]. In this work, two solution schemes are proposed and compared for the target problem.

Scheme 1. Applying the Newton-Krylov iterative method. As shown by (2.8), the resultant linear system is nonsymmetric at each Newton iteration, a nonsymmetric Krylov subspace iterative method, such as quasiminimal residual (QMR) [23], is adopted, and hence the nonsymmetric MSSOR preconditioner is used to accelerate its convergence.

Scheme 2. Compared to the nonsymmetric linear systems, solving the symmetric linear systems could lead to a saving in required memory and computer runtime. Therefore,

accelerated nonlinear solution schemes with symmetrized stiffness are attempted here, that is, at each nonlinear iteration one attempts to solve

$$\mathbf{R}(\mathbf{u}_{k-1}; \mathbf{p}_{k-1}^{ex}) + \hat{\mathbf{A}}_{k-1} \begin{bmatrix} \delta \mathbf{u}_k \\ \delta \mathbf{p}_k^{ex} \end{bmatrix} = 0, \quad (4.1)$$

and the solution vector may be updated according to (2.16). The difficulty associated with the scheme is how to construct the symmetric linear systems. In the accelerated symmetric stiffness method proposed by Chen and Cheng [24], the idea is to construct the symmetric constitutive matrix as

$$\text{sym}(\mathbf{D}_{ep}) = \mathbf{D}_e - \text{sym}(\mathbf{D}_p), \quad (4.2)$$

where $\text{sym}(\cdot)$ is a symmetrizing symbol. When $\text{sym}(\mathbf{D}_{ep}) = \mathbf{D}_e$, it corresponds to the initial stiffness (IS) method proposed by Zienkiewicz et al. [25]. When it is defined that

$$\text{sym}(\mathbf{D}_{ep}) = \mathbf{D}_{ep}^G = \mathbf{D}_e - \frac{\mathbf{D}_e \mathbf{b} \mathbf{b}^T \mathbf{D}_e}{\mathbf{b}^T \mathbf{D}_e \mathbf{b} - \mathbf{c}_G^T \mathbf{h}_G} \quad (4.3)$$

which corresponds to the so-called accelerated K_G approach. In (2.16), the step-length parameter χ_k can be determined by some optimization strategies such as the Chen's method [26] and Thomas' method [27]. Chen's method is derived by minimizing the out-of-balance load at next iteration in the least-squares sense, while the Thomas method is proposed by minimizing the "symmetric" displacement at the next iteration in the least-squares sense. In this study, the solution vector consists of coupled displacement and excess pore water pressure degrees of freedom (DOFs). The Chen method may be more straightforward to apply in this case, which will be demonstrated by the following numerical experiments. As a result, by using the present scheme, the symmetric MSSOR preconditioner may be adopted to accelerate the convergence of the SQMR solver.

4.1. Convergence Criteria

In the examples to be studied, the nonlinear iteration is terminated if the relative residual force criterion is satisfied,

$$\frac{\|\mathbf{R}_k\|_2}{\|\mathbf{F}^{\text{ext}}\|_2} \leq \text{Tol_NL} \quad \text{or} \quad k \geq \text{Maxit_NL}, \quad (k = 0, 1, \dots) \quad (4.4)$$

in which Tol_NL and Maxit_NL are the prescribed tolerance and the maximum nonlinear iterative number, respectively, and in this study Tol_NL and Maxit_NL are set as 0.01 and 50. For the employed Krylov subspace iterative method, the relative residual convergence criterion is adopted,

$$\frac{\|\mathbf{R}_{k-1} - \mathbf{A}_{k-1} [\delta \mathbf{u}; \delta \mathbf{p}^{ex}]_{k,j}^T\|_2}{\|\mathbf{R}_{k-1}\|_2} \leq \text{Tol_Lin}, \quad \text{or} \quad j \geq \text{Maxit_Lin}, \quad (j = 0, 1, \dots) \quad (4.5)$$

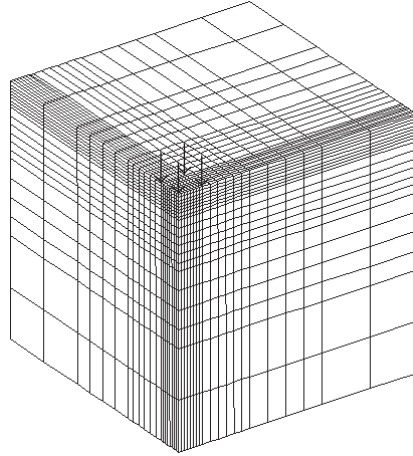


Figure 1: The $20 \times 20 \times 20$ finite element mesh of the flexible footing.

in which zero initial guess is assumed; j is the linear iterative index; Tol.Lin and Maxit.Lin are the prescribed tolerance and the maximum iterative number, respectively, and in this study Maxit.Lin is set as 50000. While to achieve a better performance for the adopted nonlinear scheme, a combined tolerance (in which Tol.Lin = $1.E - 5$ is used if the residual load is the external applied force, or Tol.Lin = $1.E - 3$ is used if the residual load is the out-of-balance force) is employed, as recommended by Chen and Cheng [24]. Based on our numerical experiences, this recommendation is reasonable because the deformation of a soil body induced by an external load is usually large and should be solved more accurately, while corrections of the deformation to resolve out-of-balance loads are relatively smaller in magnitude and hence may be solved with a less strict tolerance.

In addition, it should be mentioned that the uniform substepping method with $n_{\text{substep}} = 500$ (i.e., the number of substeps) is adopted for stress-strain integration. For more advanced automatic substepping algorithms, see Abbo [28]. In the present study, an ordinary personal computer platform equipped with a 2.4 GHz Intel Core(TM)2 Duo CPU and 3 GB physical memory is used.

4.2. Homogeneous Flexible Footing

To investigate and compare the two schemes proposed, a simple flexible footing problem with homogeneous soil material is simulated. For the homogenous soil property, the hydraulic conductivity is assumed to be $k_{s,x} = k_{s,y} = k_{s,z} = 10^{-9}$ m/s, the effective Young's modulus E' as 10 MPa, and the Poisson's ratio as $\nu' = 0.3$. The nonassociated Mohr-Coulomb soil model is used to simulate soil plasticity with the cohesion $c' = 10$ kPa, the internal friction angle $\phi' = 30^\circ$ and the dilatancy angle $\varphi = 5^\circ$. The K_0 approach is used to generate the initial field stress with $K_0 = 1 - \sin \phi'$ and soil unit weight is $\gamma = 18$ kN/m³. Due to the geometric symmetry, only a quadrant of the footing is modeled with the solution domain discretized by 8000 ($20 \times 20 \times 20$) 20-node hexahedral consolidation elements as shown in Figure 1, and the resultant total number of DOFs is 107180. For the boundary conditions, standard displacement fixities are assumed, and only the ground surface is drained. The uniform pressure load is applied on a

Table 2: Performance of different solution schemes for the flexible footing example.

Load step no.	Number of nonlinear iteration	Average iterations for each linear system	Total solution time (hours)
Scheme 1: Newton + QMR preconditioned by nonsymmetric MSSOR			
1	1	1940	0.137
2	4	1755	0.494
3	5	1756	0.624
4	5	1732	0.625
5	6	1723	0.751
Total	21	—	2.662
Scheme 2: IS (Chen) method + SQMR preconditioned by symmetric MSSOR			
1	1	1060	0.061
2	4	780	0.180
3	5	780	0.241
4	6	793	0.308
5	6	753	0.317
Total	22	—	1.129
Scheme 2: K_G (Chen) method + SQMR preconditioned by symmetric MSSOR			
1	1	1060	0.060
2	4	845	0.182
3	4	865	0.189
4	4	855	0.200
5	5	860	0.256
Total	18	—	0.903

$1 \times 1 \text{ m}^2$ area. It is increased incrementally using a total of 5 load steps. Each load increment is 0.1 MPa per second.

Table 2 provides the numerical performance of two solution schemes proposed above, that is, the Newton-Krylov (i.e., Newton-QMR) solution scheme and the Chen accelerated symmetric stiffness scheme. In the two schemes, the nonsymmetric MSSOR and symmetric MSSOR are used in conjunction with QMR and SQMR solver, respectively. Because the combined tolerance is used, the required linear iterative count for the first nonlinear iteration is higher than the following nonlinear iterations. When comparing the two schemes, it is found that the average iterative count required by MSSOR-preconditioned QMR is about two times of that required by MSSOR preconditioned SQMR solver, explaining the final results. In addition, the fact that two matrix-vector products are required in each iteration of QMR contributes to the longer computer runtime. Note that the average iterative count required by SQMR in Chen accelerated IS method is slightly smaller than that required by SQMR in Chen accelerated K_G method, indicating that the initial stiffness (i.e., the elastic stiffness) could be better conditioned. When observing the required nonlinear iterations by each scheme, it is interesting to note that three solution strategies (i.e., the Newton scheme, the Chen accelerated IS method, and Chen accelerated K_G method) exhibit similar nonlinear iterative behavior, although the Chen accelerated K_G method leads to slightly less nonlinear iterations (i.e., 18) than the other two counterparts. The exhibited similarity in nonlinear convergence indicates that the nonlinearity in the present problem is not strong. Obviously, for the homogeneous flexible footing problem the Chen accelerated K_G method coupled with

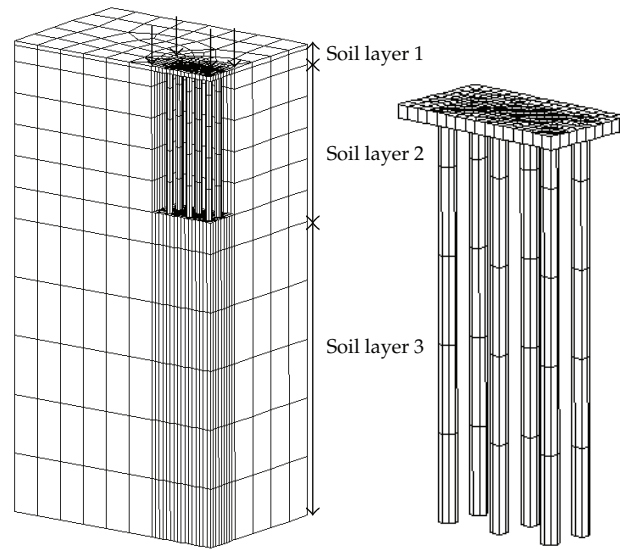


Figure 2: The finite element mesh of heterogeneous pile-group example.

Table 3: Material properties for the pile-group foundation.

Material	E' (MPa)	ν'	k (m/s)	c' (kPa)	ϕ' ($^{\circ}$)	ψ ($^{\circ}$)
Soil layer 1	20	0.3	10^{-5}	5	35	5
Soil layer 2	8	0.3	10^{-9}	50	30	8
Soil layer 3	50	0.3	10^{-6}	10	35	7
Pile and pile cap concrete	3×10^7	0.18	10^{-14}	—	—	—

MSSOR preconditioned SQMR solver may lead to a 66% reduction in total computer runtime than the Newton-QMR scheme preconditioned by nonsymmetric MSSOR. Even for the Chen accelerated IS method, a 57% reduction of total computer runtime can be achieved. It is noteworthy that the Thomas' acceleration strategy appears to be more effective in a past study [24]. However, for the coupled consolidation problem discussed in the present study, the Thomas accelerated IS method requires 1, 4, 7, 8, 8 nonlinear iterations, respectively, for the five load steps, while the Thomas accelerated K_G method takes 1, 5, 8, 6 nonlinear iterations, respectively, for the first four load steps, but it fails to converge at the last load step.

4.3. Heterogeneous Soil-Structure Interaction Example

A pile-group example is used to demonstrate the interaction between soil and structure. Because of the significant contrast in material stiffness between soils and concrete, the performance of the MSSOR preconditioner may deteriorate with the increasing contrast ratio, as noticed and investigated by Chaudhary [15]. As shown in Figure 2, the pile-group finite element mesh has total 4944 elements, in which 430 are concrete elements. The material properties for soils and concrete are tabulated in Table 3. From the table, it is seen that the concrete material is modeled by linear elastic consolidation elements with extremely small permeability, but the soils are still simulated by the Mohr-Coulomb model.

Table 4: Performance of different solution schemes for the pile-group example.

Load step no.	Number of nonlinear iteration	Average iterations for each linear system	Total solution time (hours)
Scheme 1: Newton + QMR preconditioned by nonsymmetric MSSOR			
1	4	7400	0.951
2	5	7944	1.276
3	6 (1)	13967	2.601
Total	15	—	4.823
Scheme 2: IS (Chen) method + SQMR preconditioned by symmetric MSSOR			
1	8	3300	0.464
2	13	3095	0.707
3	12	3020	0.636
Total	33	—	1.801
Scheme 2: K_G (Chen) method + SQMR preconditioned by symmetric MSSOR			
1	4	3410	0.242
2	5	3180	0.283
3	6	3284	0.349
Total	15	—	0.874

Table 4 provides numerical results of these solution schemes for the pile-group example. To be efficient for the accelerated symmetric stiffness methods, the combined tolerance introduced in Section 4.1 is still adopted. In the pile-group example, three uniform load steps are simulated and the pressure increment of 50 kPa is applied on the pile cap for a 2-day time increment. Similar to the flexible footing example, the iteration number spent by nonsymmetric MSSOR-preconditioned QMR is about two times of that of MSSOR-preconditioned SQMR solver. From the nonlinear iteration counts, it is seen that the Chen accelerated K_G method achieves a similar convergence rate as that of the Newton method, but at the third load step QMR solver dose not converge at one nonlinear iteration, which denoted by the bracketed number. Hence, at that load step the average iterative number for each linear system is remarkably increased because of $\text{Maxit_Lin} = 50000$. Compared to the Newton method, the Chen accelerated symmetric stiffness methods show better convergence behaviors, while the Chen accelerated IS method may be markedly slower than Newton method, indicating that the soil-structure interaction involving significant contrast in material stiffness may produce a stronger nonlinearity than the simple homogeneous footing problem. Upon close examination of the computer runtime, it is noticed that even though it is slower in convergence, the Chen accelerated IS method may lead to a reduction of 63% in computer runtime compared with the Newton method. When using K_G symmetric stiffness, the resultant convergence rate is similar to the Newton method, the saving in computer runtime is more impressive and a reduction of 82% may be attained. Furthermore, the Thomas acceleration scheme is examined for the initial stiffness and the K_G stiffness matrix, respectively. Both nonlinear solution strategies associated with the Thomas acceleration scheme fail, indicating that the Thomas acceleration scheme may not be suitable for problems involving coupled pore water pressure and the displacement degrees of freedom.

5. Conclusions

Soil consolidation accompanied with soil dilatancy may be frequently encountered in practice, and usually it can be modeled by nonassociated soil models. Due to the nonassociated soil model, the resultant finite element linear equation is nonsymmetric. To solve the nonsymmetric coupled Biot's linear systems of equations, two schemes in conjunction with MSSOR preconditioner are proposed and examined. Some useful observations are summarized as follows.

- (1) Two schemes are proposed for the Biot's consolidation problem involving nonassociated plasticity. Depending on the discretized linear equations, both nonsymmetric and symmetric MSSOR preconditioners are adopted for such problems,
- (2) In the accelerated symmetric stiffness methods for coupled consolidation problems, the Thomas' acceleration strategy does not exhibit better convergence behaviors as observed in the previous studies. On the other hand, the Chen's acceleration strategy is more effective, and hence it is the recommended approach for such coupled consolidation problems.
- (3) Compared to the Newton solution scheme which adopts the QMR solver preconditioned by nonsymmetric MSSOR preconditioner, the Chen accelerated symmetric stiffness approaches, which use the SQMR solver preconditioned by the symmetric MSSOR, may lead to a significant reduction in computer runtime. Based on the above numerical experiments, it may be concluded that the Chen accelerated symmetric stiffness methods have considerable potential to be exploited for solution of large-scale Biot's consolidation problems.

Acknowledgment

The research is supported in part by the Scientific Research Foundation for the Returned Overseas Chinese Scholars, State Education Ministry, no. (2010) 1561, the Fundamental Research Funds for the Central Universities, no. 2011JBM070, and the Research Fund Program of State Key Laboratory of Hydrosience and Engineering, no. SKL-2010-TC-2.

References

- [1] B. A. Cipra, "The best of the 20th century: Editors name Top 10 Algorithms," *SIAM News*, vol. 33, no. 4, pp. 1-2, 2000.
- [2] E. Chow and Y. Saad, "Experimental study of ILU preconditioners for indefinite matrices," *Journal of Computational and Applied Mathematics*, vol. 86, no. 2, pp. 387-414, 1997.
- [3] K. K. Phoon, K. C. Toh, S. H. Chan, and F. H. Lee, "An efficient diagonal preconditioner for finite element solution of Biot's consolidation equations," *International Journal for Numerical Methods in Engineering*, vol. 55, no. 4, pp. 377-400, 2002.
- [4] X. Chen, K. C. Toh, and K. K. Phoon, "A modified SSOR preconditioner for sparse symmetric indefinite linear systems of equations," *International Journal for Numerical Methods in Engineering*, vol. 65, no. 6, pp. 785-807, 2006.
- [5] I. Perugia and V. Simoncini, "Block-diagonal and indefinite symmetric preconditioners for mixed finite element formulations," *Numerical Linear Algebra with Applications*, vol. 7, no. 7-8, pp. 585-616, 2000.
- [6] V. Simoncini, "Block triangular preconditioners for symmetric saddle-point problems," *Applied Numerical Mathematics*, vol. 49, no. 1, pp. 63-80, 2004.

- [7] R. W. Freund and N. M. Nachtigal, "A new Krylov-subspace method for symmetric indefinite linear systems," in *Proceedings of the 14th IMACS World Congress on Computational and Applied Mathematics*, W. F. Ames, Ed., pp. 1253–1256, Atlanta, Ga, USA, 1994.
- [8] C. Keller, N. I. M. Gould, and A. J. Wathen, "Constraint preconditioning for indefinite linear systems," *SIAM Journal on Matrix Analysis and Applications*, vol. 21, no. 4, pp. 1300–1317, 2000.
- [9] Z.-Z. Bai, M. K. Ng, and Z.-Q. Wang, "Constraint preconditioners for symmetric indefinite matrices," *SIAM Journal on Matrix Analysis and Applications*, vol. 31, no. 2, pp. 410–433, 2009.
- [10] K.-C. Toh, K.-K. Phoon, and S.-H. Chan, "Block preconditioners for symmetric indefinite linear systems," *International Journal for Numerical Methods in Engineering*, vol. 60, no. 8, pp. 1361–1381, 2004.
- [11] L. Bergamaschi, M. Ferronato, and G. Gambolati, "Mixed constraint preconditioners for the iterative solution of FE coupled consolidation equations," *Journal of Computational Physics*, vol. 227, no. 23, pp. 9885–9897, 2008.
- [12] M. Ferronato, L. Bergamaschi, and G. Gambolati, "Performance and robustness of block constraint preconditioners in finite element coupled consolidation problems," *International Journal for Numerical Methods in Engineering*, vol. 81, no. 3, pp. 381–402, 2010.
- [13] J. B. Haga, H. Osnes, and H. P. Langtangen, "Efficient block preconditioners for the coupled equations of pressure and deformation in highly discontinuous media," *International Journal for Numerical and Analytical Methods in Geomechanics*, vol. 35, no. 13, pp. 1466–1482, 2011.
- [14] C. Janna, M. Ferronato, and G. Gambolati, "A block Fesai-Ilu parallel preconditioner for symmetric positive definite linear systems," *SIAM Journal on Scientific Computing*, vol. 32, no. 5, pp. 2468–2484, 2010.
- [15] K. B. Chaudhary, *Preconditioners for soil-structure interaction problems with significant material stiffness contrast*, Ph.D. thesis, National University of Singapore, 2010.
- [16] R. S. Dembo, S. C. Eisenstat, and T. Steihaug, "Inexact Newton methods," *SIAM Journal on Numerical Analysis*, vol. 19, no. 2, pp. 400–408, 1982.
- [17] P. N. Brown and Y. Saad, "Convergence theory of nonlinear Newton-Krylov algorithms," *SIAM Journal on Optimization*, vol. 4, no. 2, pp. 297–330, 1994.
- [18] M. A. Biot, "General theory of three-dimensional consolidation," *Journal of Applied Physics*, vol. 12, no. 2, pp. 155–164, 1941.
- [19] I. M. Smith and D. V. Griffiths, *Programming the Finite Element Method*, John Wiley & Sons, Chichester, UK, 2nd edition, 1988.
- [20] S. C. Eisenstat, "Efficient implementation of a class of preconditioned conjugate gradient methods," *SIAM Journal on Scientific and Statistical Computing*, vol. 2, no. 1, pp. 1–4, 1981.
- [21] P. A. Vermeer and R. de Borst, "Non-associated plasticity for soils, concrete and rock," *Heron*, vol. 29, no. 3, pp. 1–62, 1984.
- [22] O. C. Zienkiewicz, C. Humpheson, and R. W. Lewis, "Associated and non-associated visco-plasticity and plasticity in soil mechanics," *Geotechnique*, vol. 25, no. 4, pp. 671–689, 1975.
- [23] R. W. Freund and N. M. Nachtigal, "QMR: a quasi-minimal residual method for non-Hermitian linear systems," *Numerische Mathematik*, vol. 60, no. 3, pp. 315–339, 1991.
- [24] X. Chen and Y.-G. Cheng, "On accelerated symmetric stiffness techniques for non-associated plasticity with application to soil problems," *Engineering Computations*, vol. 28, no. 8, pp. 1044–1063, 2011.
- [25] O. C. Zienkiewicz, S. Valliappan, and I. P. King, "Elasto-plastic solutions of engineering problems "initial stress", finite element approach," *International Journal for Numerical Methods in Engineering*, vol. 1, no. 1, pp. 75–100, 1969.
- [26] C. N. Chen, "Efficient and reliable accelerated constant stiffness algorithms for the solution of non-linear problems," *International Journal for Numerical Methods in Engineering*, vol. 35, no. 3, pp. 481–490, 1992.
- [27] J. N. Thomas, "An improved accelerated initial stress procedure for elasto-plastic finite element analysis," *International Journal for Numerical and Analytical Methods in Geomechanics*, vol. 8, no. 4, pp. 359–379, 1984.
- [28] A. J. Abbo, *Finite element algorithms for elastoplasticity and consolidation*, Ph.D. thesis, University of Newcastle, 1997.



Hindawi

Submit your manuscripts at
<http://www.hindawi.com>

